Effect of 3-aminopropyltriethoxysilane and *N,N*-Dimethyldodecylamine as Modifiers of Na^+-Montmorillonite on SBR/Organoclay Nanocomposites

Wook-Soo Kim,[1] Juhui Yi,[1] Dong-Hyun Lee,[1] Il-Jin Kim,[2] Woo-Jung Son,[2] Jong-Woo Bae,[3] Wonho Kim[1]

[1]*Department of Chemical Engineering, Pusan National University, Busan 609-735, Korea*
[2]*R&D Center, Dongil Rubber Belt Co., Ltd., Busan 609-721, Korea*
[3]*Rubber Material Research Division, Korea Institute of Footwear and Leather Technology, Busan 614-100, Korea*

Received 22 April 2009; accepted 25 November 2009
DOI 10.1002/app.31861
Published online 22 February 2010 in Wiley InterScience (www.interscience.wiley.com).

ABSTRACT: In this study, styrene butadiene rubber (SBR)/organoclay nanocomposites were manufactured using the latex method with 3-aminopropyltriethoxysilane (APTES) and *N,N*-dimethyldodecylamine (DDA) as modifiers. The layer-to-layer distance of the silicates was observed according to each manufacturing process for APTES as the modifier using the X-ray diffraction (XRD) method. From the XRD results and the TEM images, the dispersion of the silicates impoved for both APTES-MMT and DDA-MMT, and the dispersion of the silicates with the DDA modifier improved more than the APTES modifier. The SBR/DDA-MMT compound exhibited the fastest scorch time, optimal vulcanization time, and cure rate. The dynamic viscoelastic properties of the SBR/APTES-MMT compound were measured according to the change in the strain amplitude in order determine if a covalent bond was formed between APTES and bis(triethoxysilyl-propyl)-tetrasulfide (TESPT). The mechanical properties of the SBR/DDA-MMT nanocomposite improved more than the SBR/APTES-MMT composite because the vulcanization effects of alkylamine and the dispersion of silicates within the rubber matrix were relatively good. © 2010 Wiley Periodicals, Inc. J Appl Polym Sci 116: 3373–3387, 2010

Key words: SBR; organoclay; latex method; XRD; cure rate; dispersion

INTRODUCTION

Most nonpolar rubbers, such as natural rubber (NR), butadiene rubber (BR), and styrene butadiene rubber (SBR) are widely used for commercial products and show a high compatibility with hydrophobic reinforcing fillers such as carbon black, etc.[1,2] However, silica or layered silicates do not evenly distribute into the nonpolar rubber matrix and do not exhibit a sufficient reinforcing effect with the filler itself because the interaction between the hydrophobic rubber matrix and the hydrophilic filler is weak.[3-8] Montmorillonite (MMT) is the most commonly used clay, and the structure of MMT consists of one octahedral aluminum sheet sandwiched between two tetrahedral sheet in a layered asssembly.[9] The stacking of the silicate layers causes a van der Waals gap between the layers called a gallery. For Na^+-MMT, isomorphic substitution within the octahedral layers of MMT, for example Al^{3+} replaced by Mg^{2+}, causes negative charges within the compound that are counterbalanced by the Na^+ ions residing in the interlayer.

The silicate in the plate-like structure has an aspect ratio of over 100, along with a layer thickness of 1 nm and side length of 100–1000 nm. When these layered silicates are distributed to each layer, they tend to have a large specific surface area.[9] A high level of reinforcement can be obtained from a small amount of silicates because of these characteristics. Additionally, the decreased gas permeability, the increased heat distortion temperature, and the decreased flammability of the nanoclay filled composites originated from the plate-like structure of the silicates.[10] In case of the layered silicates, the dispersion of the layered silicates within the rubber matrix can largely be divided into three categories.[11] In the first case, the polymer chains wet the surface of the MMT aggregates. In the second case, the polymer chains are intercalated into the clay galleries, and in the third case, each MMT aggregate layer is completely exfoliated to a plate-like shape within the successive polymer matrix.

The dispersion or exfoliation of the silicate layers in rubber matrix can be classified into four methods, the solution method, the polymerization method, the

Correspondence to: W. Kim (whkim@pnu.edu).
Contract grant sponsor: Korea Research Foundation [Korean Government (MOEHRD)]; contract grant number: KRF-2007-313-D00234.
Contract grant sponsor: Brain Korea 21 Project.

compounding method and the latex method. Using the latex method,[10,12-19] the polarity of the silicate surface can be decreased through the addition of alkylamine or alkylammonium after the clay swells in a suspension of clay and water. Then the silicates can be reaggregated through mixing with rubber latex. This process can be controlled through the addition of a coagulant according to the organification of the silicates in the follow-up coagulation process.[7,8] Most of the recent studies have focused on improving the dispersion or exfoliation of the silicates using alkyl ammonium ions as modifiers. Additionally, the interaction of the modified silicates with rubber molecules is weak for the alkyl ammonium ions because the van der Waals force is the main interaction. If the strong chemical bonding between silicates and rubber molecules can be obtained, the reinforcement effect of rubber using intercalated or exfoliated silicates is expected to be very large if a strong chemical bond can be formed between the silicates and the rubber molecules.

According to a study by Jia et al.,[8] a SBR/organoclay compound was manufactured from the generation of a large quantity of hydroxyl groups on the surface of silicates using the latex method with 3-aminopropyltriethoxysilane (APTES) as a modifier. The addition of TESPT to the manufactured compound resulted in 300% modulus, which was eight times greater than the pure SBR compound because the improved interfacial interaction between the rubber molecules and the silicates created a strong covalent bond between the hydroxyl groups that were generated from APTES and the ethoxy group of TESPT. According to the results, SBR/silica/clay nanocomposites were developed in this study using the latex method with *N*,*N*-dimethyldodecylamine (DDA) as a modifier. The dispersion of the silicates within the rubber matrix improved, and thereby, the mechanical properties of the SBR nanocomposites also improved.[19]

In this study SBR/organoclay nanocomposites were prepared using the latex method and the effects of APTES-MMT and DDA-MMT on the SBR/organoclay nanocomposites were examined by evaluating the layer distance, the dispersion of the silicates, and the behaviors of the cure characteristics, swelling ratio, morphology, mechanical properties, and dynamic viscoelastic properties.

EXPERIMENTAL

Materials

In this experiment, SBR 1502 (bound styrene contents: 23.5% in SBR; 25 wt % of solid contents in the latex; Kumho Petrochemical, Korea) was used for the SBR latex and KUNIPIA-F (cation exchange capacity; 115 mequiv./100g; Kunimini, Japan) was used for the sodium montmorillonite (Na^+-MMT). 3-Aminopropyltriethoxysilane (APTES, 99%) and *N*,*N*-dimethyldodecylamine (DDA, 97%) were purchased from Aldrich and used to modify Na^+-MMT, and bis(triethoxysilylpropyl)tetrasulfide (TESPT) was used as a coupling agent. Their chemical structures of the compounds are shown in the Figure 1. Additionally, zinc oxide (ZnO), stearic acid, antioxidant (BHT; 2,6-di-*tert*-butyl-4-methyl-phenol), sulfur and accelerator (TBBS; *N*-*tert*-butyl-2-benzothiazol sulfonamide) were used as additives.

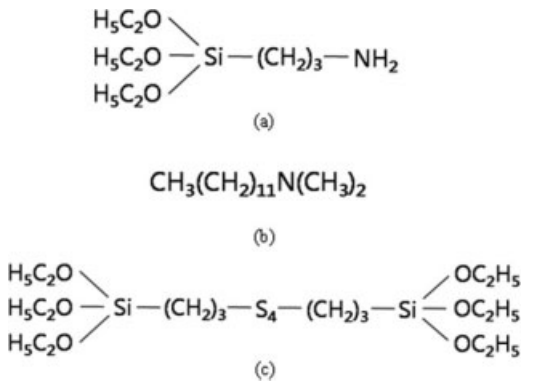

Figure 1 Chemical structures of (a) the APTES, (b) the DDA, and (c) the TESPT.

Modifier-MMT suspension solutions

First, 7 g of Na^+-MMT was stirred in 700 mL of distilled water for 24 h at 65°C. The 2 g each of APTES and DDA were added to 200 mL of distilled water and stirred for 10 h at 50°C. These two solutions were mixed and intensively stirred for 15 h at 65°C.

Co-coagulation of SBR latex/modifier-MMT

To prepare the SBR/organoclay compound, the modifier-MMT suspension and 420 g of SBR latex were stirred for 30 min at room temperature. A coagulation solution was prepared by mixing 5.6 mL of sulfuric acid (latex coagulant) with 500 mL of distilled water. Then this solution was added to the mixed solution of SBR latex and the modifier-MMT suspension, which coagulated the latex. The SBR compound was prepared by adding APTES or DDA to 420 g of SBR latex and stirring the mixture for 30 min at room temperature. Then the latex coagulant was added to the SBR latex. The prepared SBR and SBR/organoclay compounds were washed until the pH reached a value 7, and then they were dried in a dry oven for 24 h at 75°C.

Manufacturing of SBR nanocomposites

Each of the SBR and SBR/organoclay compounds were mixed in an 8-inch two-roll mill (rotor speed

ratio; 1 : 1.4) for 3 min at 50°C, and TESPT was added to the prepared compound and mixed in a banbury type kneader for an additional 8 min at 110°C. On the other hand, the compound that did not contain TESPT was mixed in the kneader for 11 min. Then the primary additives such as ZnO, stearic acid and BHT were added with mixing for 4 min. At this time, the dump temperature ranged from 130 to 135 °C. Additionally, the secondary additives, such as sulfur as the crosslinker and TBBS as the accelerator, were added, and the compound was mixed for 3 min at 40°C using a two-roll mill to prevent scorching due to the viscous heat generation of the compound.

The optimal vulcanization time (t_{90}) was determined by measuring the torque value of the rubber compound at 160°C using an oscillating disk rheometer (ODR, MYUNG-JI Tech, Korea, Model; ODR 2000). Then the mixed compounds were pressed at 2000 psi and 160°C using a hydraulic press at for the appropriate vulcanization time (t_{90}) to manufacture the SBR nanocomposites.

Layer-to-layer structure analysis of organoclay

The layer-to-layer distance of the organoclay was measured using an X-ray diffraction (XRD) test at room temperature with a Rigaku D/MAX 2200 (Japan) X-ray diffractometer with Cu-Kα radiator. The XRD data were obtained from 1 to 10° (2θ) at a rate of 1°/min.

Cure characteristics

The cure characteristics of the rubber compounds were measured using the ODR under the following conditions: oscillation angle; ±1°, temperature; 160°C, and running time; 40 minutes.

Measurement of swelling ratio

The degree of crosslinking of the vulcanized rubber compounds were determined from the swelling ratio measurements. The weight of the specimens was measured after the 30 × 5 × 2 mm specimen was impregnated into a toluene solution for 1, 2, 3, 6, 9, 12, and 24 h at 30°C according to the ASTM D 471–79. Then the swelling ratio (%) was determined using the following expression with respect to the measured weight of the specimens.

$$Q\,(\%) = \frac{(W_1 - W_0)/d_2}{W_0/d_1} \times 100$$

Q: swelling ratio (%)
W_0: weight of the specimen before swelling
W_1: weight of the specimen after swelling
d_1: density of SBR (0.94 g/mL)
d_2: density of toluene (0.87 g/mL)

Morphology

The specimens were microtomed up to a thickness of 70 nm in a liquid nitrogen atmosphere and then TEM (transmission electron microscopy; JEOL, Japan, Model; JEM2100F) images were obtained at an acceleration voltage of 200 kV to examined the dispersion and exfoliation states of the organoclay in the matrix.

Mechanical properties

Dumbell-shaped specimens (100 × 25 × 2 mm; gauge length 20 mm and gauge width 5 mm) were cut from a flat sheet using a single stroke to ensure that the substance was smooth. The mechanical properties, such as the moduli at 100 and 300% elongation, the tensile strength and the elongation at break, were examined at an applied extension speed of 500 mm/min using a load cell of 5000 N in a Universal Testing Machine (UTM, KSU, Korea, Model; KSU-05M-C) according to the ASTM D412.

Analysis of the dynamic viscoelastic behavior

For the SBR/organoclay compound with APTES, silanization was assumed to occur between the hydroxyl group of APTES and the ethoxy group of TESPT during mixing in the banbury type kneader. The storage modulus (E') was measured with respect to the strain sweep of the uncured SBR/organoclay compound at a frequency of 1 Hz and a temperature of 60°C in the tension film mode using DMA (TA Instruments, Model; RSA III) to determine the effects of TESPT. These measurements were performed with an increasing strain amplitude from 0.1 to 40%.

The storage modulus (E') and tan δ of the cured SBR/organoclay compound were measured using the tensile film mode of a DMA (TA Instruments, Model; DMA Q800 V7.1 Build 116) with an amplitude of 30 μm and a frequency of 10 Hz at a temperature sweep of 5°C/min from −60 to 80°C.

RESULTS AND DISCUSSION

Layer-to-layer structure analysis of silicates according to the manufacturing process of SBR/organoclay compounds

Figure 2 shows the XRD analysis that was performed to understand the layer-to-layer structure of the silicates in the SBR/organoclay nanocomposites that were manufactured using the latex method. The suggested silicate states for each process are illustrated in Figure 3. The compound formulations for

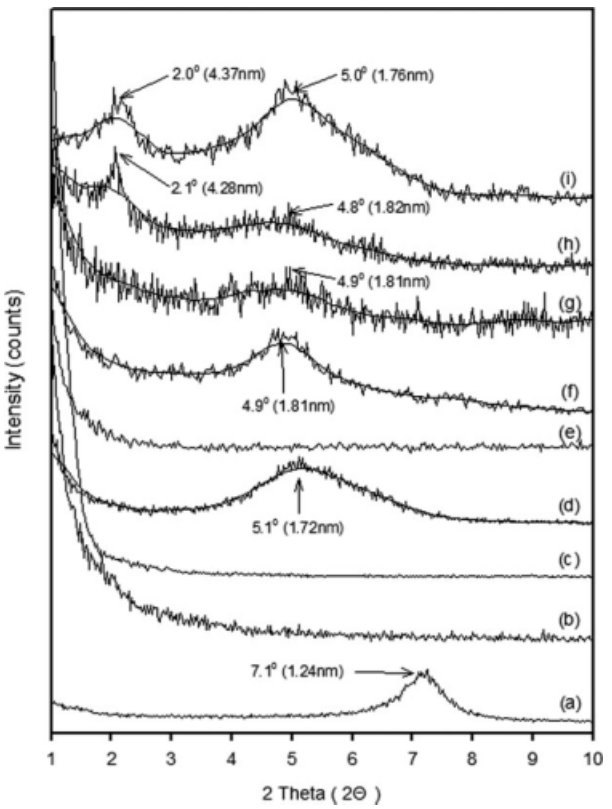

Figure 2 X-ray diffraction patterns at various stages of the preparation process: (a) Na^+-MMT; (b) Na^+-MMT + water (swelling total mixing time 24 hr); (c) Na^+-MMT + APTES + Water; (d) APTES-MMT (dried); (e) Na^+-MMT + APTES + water + SBR Latex; (f) after coagulation with sulfuric acid; (g) after coagulation(dried); (h) after compounding (include additives and TESPT); and (i) after vulcanization.

the SBR/organoclay nanocomposites are shown in the Table I, and the activator, accelerator and sulfur concentrations were set to the standard nonoil type formulation according to the ASTM D3185. In Figure 2(a) the layer-to-layer distance of pure Na^+-MMT was 1.24 nm (7.1°). The clay was swelled in distilled water for 24 h at 65°C to exfoliate the clay in an aqueous solution, which was confirmed by the disappearance of the peak in the range of 2θ in Figure 2(b). Figure 2(c) shows the XRD results for addition of the APTES solution to the MMT-suspension to form the organoclay. No peak appeared in the XRD pattern, and an organoclay state was observed in Figure 3(c) for mixture of the suspension and APTES solution. The APTES-MMT suspension was filtered using filter paper with a pore size of 5 μm to identify the physical adsorption between APTES and the silicate. A similar experiment was carried out for the DDA-MMT suspension. A clay cake formed on the filter paper for APTES-MMT suspension, whereas the clay cake was not observed for the DDA-MMT suspension solution. From the XRD analysis in Figure 2(d), the layer-to-layer distance for APTES-MMT was 1.72 nm (5.1°). The clay cake formed and APTES intercalated between the layers of clay because APTES had a polar hydroxyl group that was generated through the hydrolysis of the ethoxy group. As this transition occurred, the physical adsorption between APTES and the silicates was either caused by hydrogen bonding between the hydroxyl groups of APTES and the oxygen atoms in the silicate or the ion-dipole interaction between APTES and the ions that existed between the silicate layers. Jia et al. compared the FTIR peak of the OH functional group

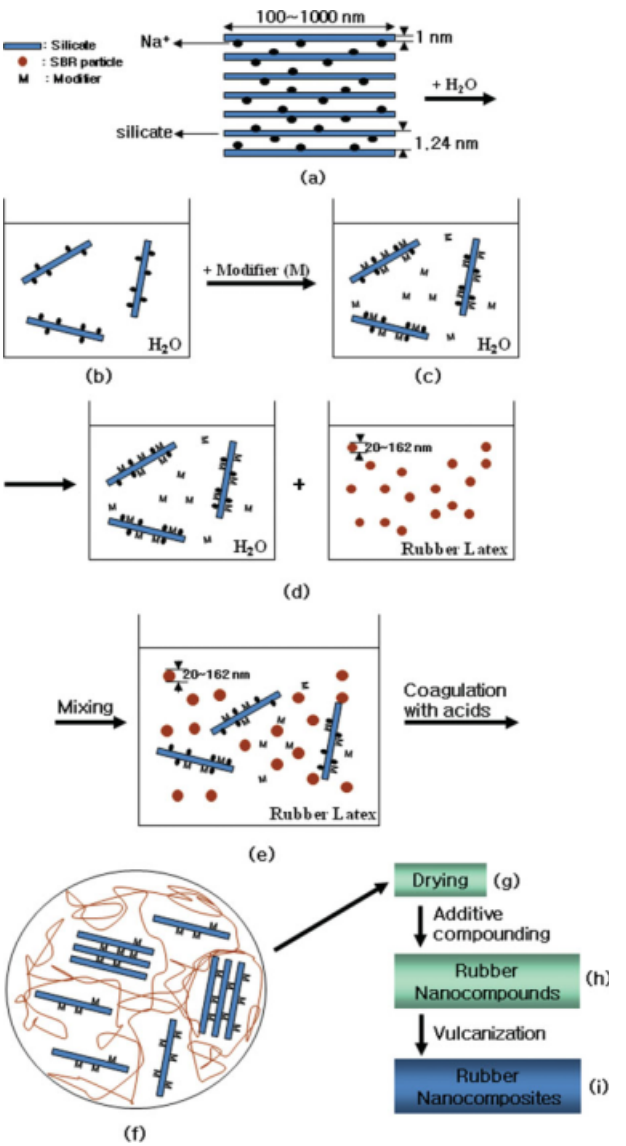

Figure 3 Suggested silicate states during the A-5 compound preparation process: (a) Na^+-MMT; (b) Na^+-MMT + water (swelling total mixing time 24 hr); (c) Na^+-MMT + APTES + water; (d) and (e) APTES + MMT + SBR latex; (f) after coagulation with sulfuric acid; (g) after coagulation (dried); (h) after compounding (with additives and TESPT); and (i) after vulcanization. [Color figure can be viewed in the online issue, which is available at www.interscience.wiley.com.]

TABLE I
Experimental Formulation of the SBR and SBR/Clay Compounds for the Filled System [Amounts; Weight Parts Per 100 Weight Parts of Rubber (phr)]

Materials	A-1	A-2	A-3	A-4	A-5	A-6
SBR 1502			100			
Clay	–	7	7	7	7	7
APTES	–	–	–	2	2	–
DDA	–	–	–	–	–	2
TESPT	–	–	2	–	2	2
Zinc oxide			3			
Stearic acid			1			
BHT			1			
TBBS			1			
Sulfur			1.75			
t_{10} (min: sec)	20 : 12	6 : 33	6 : 56	7 : 46	6 : 35	5 : 50
t_{90} (min: sec)	31 : 06	31 : 38	31 : 24	27 : 16	26 : 00	21 : 18
t_{90}–t_{10} (min: sec)	10 : 54	25 : 05	24 : 28	19 : 30	19 : 25	15 : 28
Cure rate (N-m/min)	0.168	0.034	0.049	0.082	0.093	0.158
T_{min} (N-m)	0.50	0.90	0.78	0.75	0.61	0.52
T_{max} (N-m)	2.33	1.76	1.99	2.35	2.41	2.96
T_{max}–T_{min} (N-m)	1.83	0.86	1.21	1.60	1.80	2.44

at a wave number of 3624 cm^{-1} for pure Na$^+$-MMT and APTES-MMT.[8] This comparision showed that a large quantity of hydroxyl groups were generated on the surface of the clay when APTES was added.[8] Figure 3(e) shows the SBR latex mixed into the APTES-MMT suspension solution and no XRD peaks appeared in Figure 2(e). These XRD results were examined to determine if the SBR particles and emulsifier caused aggregation in the silicates. Hence, the SBR latex did not have an influence on the layer-to-layer structure of the silicates. Sulfuric acid was used as a coagulant to obtain a crumb phase for the SBR/organoclay compound in Figure 3(f), and at the same time, a cation exchange reaction occurred between the APTES ammonium ion and the Na$^+$ ion of the silicate. Accordingly, the manufacturing process for SBR/organoclay nanocomposite was simplified when these two procedures were performed at the same time. Two factors influenced the layer-to-layer structure during the coagulation process. First, the H$^+$ ion was used as a coagulant, and the ammonium ions of APTES and the H$^+$ ions coexisted in between the silicate layers after the cation exchange reaction with the Na$^+$ ions. Therefore, more intercalated H$^+$ ions could possibly have formed compared to intercalated APTES because of the high concentration of H$^+$ ions. On the other hand, the intercalated SBR particles in between the silicate layers could have influenced the structural properties. In Figure 2(f), the layer-to-layer distance upon coagulation increased more than the value of 1.81 nm (4.9°) for pure Na$^+$-MMT, the APTES ammonium ions were intercalated in between the layers of the silicates through the cation exchange reaction with the Na$^+$ ions of clay. Figure 4(a) has an XRD peak at 6.3° (1.40 nm) for the SBR/Na$^+$-MMT compound that was made through coagulation with sulfuric acid. Accordingly, the large concentration of H$^+$ ions did not impede the cation exchange reaction between the ammonium ions of APTES and the Na$^+$ ions of clay. A process must be used to remove the remaining acid on the surface of organoclay when the clay was manufacture through the ammonification of the modifier with an acid.

Additionally, the particle size distribution of the SBR latex was determined using a particle size analyzer to determine if the SBR particles were intercalated in between the silicate layers. The results showed that the particle size distribution was 20–162 nm, and the average particle size was 78 nm.

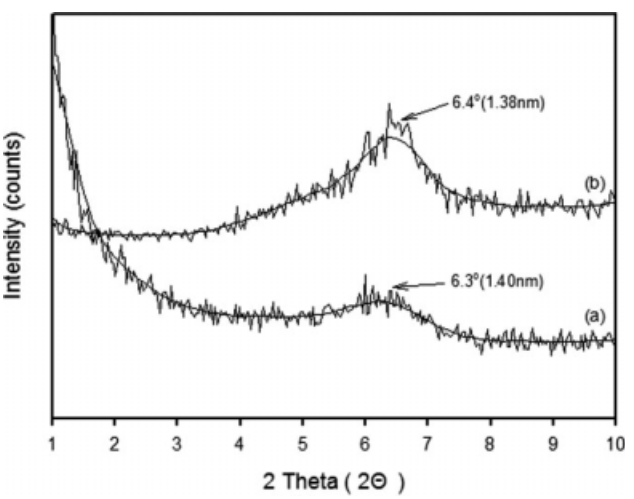

Figure 4 X-ray diffraction (XRD) patterns of the A-2 compound after (a) coagulation (dry sample) and (b) vulcanization.

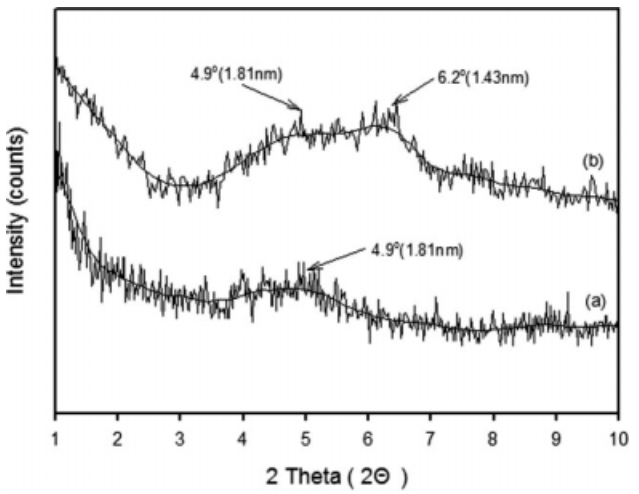

Figure 5 X-ray diffraction (XRD) patterns of the (a) A-5 and (b) A-6 compounds after coagulation (dry sample).

Therefore, an intercalating structure between the layers of the silicates was not easily formed while maintaining the stability of the SBR particles. In Figure 2(g), the layer-to-layer distance was 1.81 nm (4.9°) for the dried compound that had its moisture removed after coagulation. This distance was identical to the specimen before drying. After adding the activating agent, the accelerator and sulfur to the compound in a two-roll mill, two peaks appeared at 4.8° (1.82 nm) and 2.1° (4.28 nm) in Figure 2(h). Stearic acid was used as an activator to penetrate into the galleries of the organoclay.[20] Therefore a peak appeared because of the longer layer-to-layer distance. The XRD pattern in Figure 2(i) after vulcanization exhibited the same two peaks as Figure 2(h) before vulcanization.

Figures 5 and 6 show the XRD data for the silicate layer-to-layer structure of the SBR/organoclay compounds with APTES (A-5 compound) and DDA (A-6 compound) after coagulation and after vulcanization, respectively. Figure 5(a) shows the XRD data of the A-5 compound. In this figure, the layer-to-layer distance increased by 0.41 nm compared to the A-2 compound filled with the clay because of APTES intercalated in between the layers of the silicates. In Figure 5(b), two peaks at 1.81 nm (4.9°) and 1.43 nm (6.2°) appeared for the A-6 compound with DDA as the modifier. Therefore the H^+ ions that were used as a coagulant competed with the ammonium ions of DDA that were intercalated in between the layers of the silicates. The H^+ ions more easily intercalated in between the layers of the silicates than the ammonium ions of DDA because of the long carbon chain length, with a peak at 6.2°, which matched the 6.3° peak in Figure 4(a) for the A-2 compound with clay.

For the XRD data of SBR/organoclay after vulcanization in Figure 6, two peaks were observed for the A-5 compound at 4.37 nm (2.0°) and 1.76 nm (5.0°), and two peaks were also observed for the A-6 compound at 3.92 nm (2.2°) and 1.37 nm (6.4°). The peaks at 1.76 nm (5.0°) for the A-5 compound and 1.37 nm (6.4°) for the A-6 compound corresponded to the decrease in the layer-to-layer distance after vulcanization. The new peaks at 4.37 nm (2.0°) for the A-5 compound and 3.92 nm (2.2°) for the A-6 compound corresponded to the penetration of stearic acid into the galleries of APTES-MMT and DDA-MMT, respectively. The morphology was examined through the TEM analysis to investigate the dispersion of the silicates in the rubber matrix.

Cure characteristics of SBR and SBR/clay compounds

The cure characteristics of the unfilled SBR compounds are shown in the Figure 7 according to the formulations in Table II to determine the influence of the APTES and DDA modifiers on the clay. The

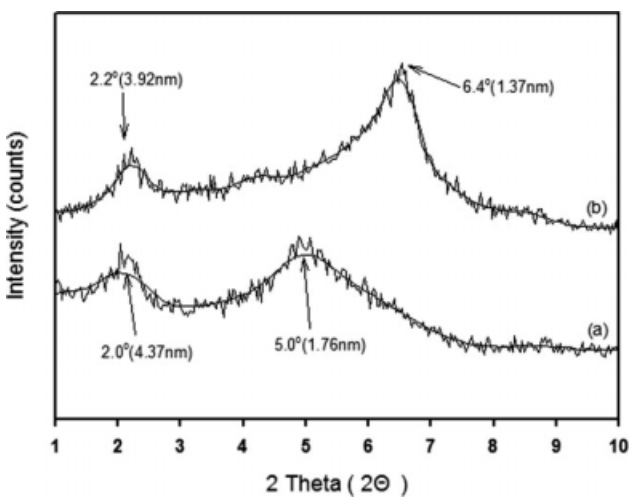

Figure 6 X-ray diffraction (XRD) patterns of the (a) A-5 and (b) A-6 compounds after vulcanization.

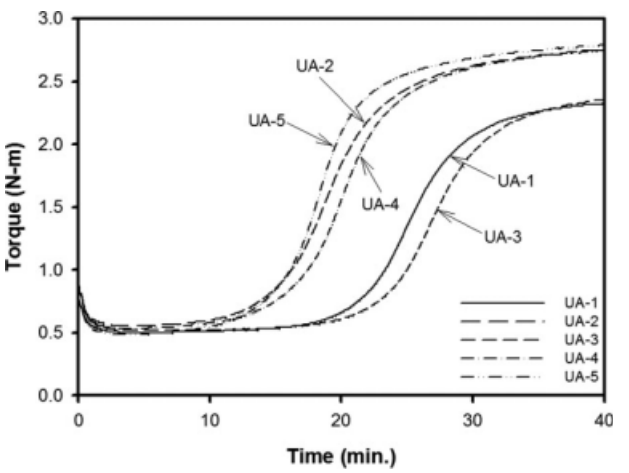

Figure 7 Cure characteristics of the various compounds for the unfilled system.

TABLE II
Experimental Formulation of the SBR Compounds for the Unfilled System [Amounts; Weight Parts Per 100 Weight Parts of Rubber (phr)]

Materials	UA-1	UA-2	UA-3	UA-4	UA-5
SBR 1502			100		
APTES	–	–	2	2	–
DDA	–	–	–	–	2
TESPT	–	2	–	2	2
Zinc oxide			3		
Stearic acid			1		
BHT			1		
TBBS			1		
Sulfur			1.75		
t_{10} (min: sec)	20 : 12	13 : 56	22 : 00	14 : 48	13 : 35
t_{90} (min: sec)	31 : 06	26 : 49	32 : 35	27 : 13	24 : 42
t_{90}–t_{10} (min: sec)	10 : 54	12 : 53	10 : 35	12 : 25	11 : 07
Cure rate (N-m/min)	0.168	0.171	0.173	0.178	0.207
T_{min} (N-m)	0.50	0.55	0.52	0.53	0.49
T_{max} (N-m)	2.33	2.76	2.35	2.76	2.79
T_{max}–T_{min} (N-m)	1.83	2.21	1.83	2.22	2.30

concentrations of the activator, the accelerator and sulfur were set to the standard nonoil type formulation of ASTM D3185.

The scorch time (t_{10}) and optimal vulcanization time (t_{90}) of the unfilled SBR compounds decreased in the order of UA-3 > UA-1 > UA-4 > UA-2 > UA-5. The scorch time and optimal vulcanization time of the UA-2 compound become faster than the UA-1 compound through the addition of TESPT. The vulcanization rate increased as the tetrasulfide group of TESPT participates in the crosslink of SBR.[4] The UA-3 compound with APTES had the slowest scorch time and optimal vulcanization time because the ethoxy group of APTES transformed into the hydroxyl group through the hydrolysis reaction in water. Some of the accelerator hydrogen bonded with the hydroxyl group of APTES and therefore, could not participate in the crosslinking, in turn delaying the crosslinking reaction.[8,21] The UA-5 compound with both DDA and TESPT exhibited the fastest scorch time and optimal vulcanization time because the accelerator and the amino group of DDA promoted the ring-opening rate of sulfur (S_8).[22] On the other hand, the scorch time and optimal vulcanization time of the UA-4 compound with both APTES and TESPT were slightly delayed compared to the UA-2 compound. These results were similar to the UA-3 compound, where the accelerator bonded with the hydroxyl group of APTES and could not participate in the crosslink reaction, which in turn, delayed the reaction.

The cure rate increased in the order of UA-1 < UA-2 < UA-3 < UA-4 < UA-5. Although, the scorch time and optimal vulcanization time of the UA-3 compound were the slowest, the cure rate exhibited a different tendency. The scorch time was delayed because of the influence of the hydroxyl group of APTES, but, the cure rate was slightly faster as the amine group of APTES promoted the ring-opening rate of sulfur (S_8). The cure rates of the UA-4 and UA-5 compounds were faster than the UA-2 compound because the amino groups of DDA and APTES improved the curing even though DDA exhibited better crosslinking than APTES. These results showed the compound with DDA did not exhibit the same accelerator loss that the hydroxyl group of APTES caused.

The maximum torque of the unfilled SBR compound increased in the order of UA-1 < UA-3 < UA-2 = UA-4 < UA-5, and the delta torque [maximum torque (T_{max}) – minimum torque (T_{min})] increased in the order of UA-1 = UA-3 < UA-2 ≈ UA-4 < UA-5. The maximum torque value of the UA-3 compound only increased only by 0.9% over the UA-1 compound, and therefore, the chemical reaction between APTES and the SBR molecules was negligible. The maximum torque and the delta torque of the UA-2 compound increased by 15.6 and 17.2%, respectively, compared to the pure SBR compound. The crosslinking increased because the tetrasulfide group of TESPT was involved in the vulcanization process.[4] The maximum torque and delta torque of the UA-5 compound with DDA increased by 1.1 and 3.5%, respectively, compared to the UA-4 compound with APTES. Similar to the cure characteristics of the UA-5 compound, the compound with DDA showed a higher degree of crosslinking than APTES because DDA did not have the accelerator loss that the hydroxyl group of APTES caused. Accordingly, the UA-5 compound exhibited the highest crosslinking effects.

The cure characteristics of the SBR/organoclay compounds filled with clay are shown in Figure 8

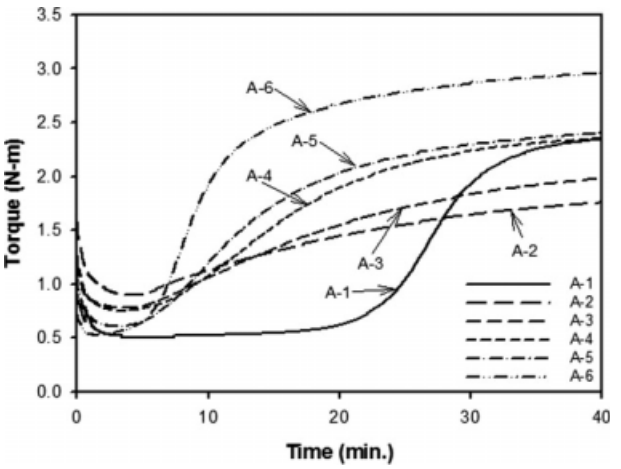

Figure 8 Cure characteristics of the various compounds for the filled system.

and Table I. The scorch time of the various compounds increased in the order of A-6 < A-2 ≈ A-5 < A-3 < A-4 < A-1. The scorch times were faster for the filled compounds compared to the unfilled SBR compounds. The acidity of the MMT-suspension was measured to examine its effect on the ring-opening rate of sulfur, the acidity pH was about 9.4, showing a weak alkalinity for MMT. Accordingly, these alkalinity results[23] were attributed to the crosslinking characteristics of the SBR rubber with the clay and the heat transfer effect of the plate-like shape of the silicates with a relatively wide surface area compared to the thickness of the clay. However, the scorch time was slightly delayed for the A-4 compound compared to the A-2 and A-3 compounds. A large number of hydroxyl groups were generated on the silicate surface by the APTES modifier, and the bonding between the accelerator and the hydroxyl groups delayed the vulcanization rate.[8,21] These results were identical to the scorch time delay results that were caused by the addition of APTES to the unfilled SBR compound. On the other hand, the scorch time of the A-5 compound was similar to the A-2 and A-3 compounds. These results showed that a crosslinking delay effect was not exhibited as the amount of hydroxyl groups created on the clay surface by APTES reduced through the silanization reaction with the ethoxy group of TESPT. Additionally, the A-6 compound exhibited the fastest scorch time because the crosslinking reaction was promoted by the amine group of DDA. Amino group is known to promote the crosslinking reaction of the SBR and NR compounds.[24]

The cure rate increased in the order of A-2 < A-3 < A-4 < A-5 < A-6 < A-1. This trend was different than the unfilled system, where the cure rate increased when APTES, DDA and TESPT were added. The cure rates of the SBR/clay compounds were slower than that the unfilled SBR compounds. Therefore, the cure rate was influenced by the filler, and some of the accelerator did not participate in the crosslinking reaction because the hydrophilic accelerator adsorbed onto the layer-to-layer structure of the clay. The optimal vulcanization time and cure rate of the A-4, A-5, and A-6 compounds that used a modifier were faster than the A-2 and A-3 compounds that did not use a modifier because the polarity of the silicates reduced as the modifier was inserted in between the layers of the silicates, and the dispersion of the silicates improved within the rubber matrix. Accordingly, the accelerator loss was reduced because the modifier caused a less polar aggregate or agglomerate structure for the silicates. Additionally, the cure rate of the modified compounds was faster than the SBR/clay compound without organic treatment because the amino groups of APTES and DDA promoted crosslinking. Especially for the A-6 compound, the crosslinking effect of the amino group was about 1.7 times higher than the A-5 compound because DDA did not exhibited the accelerator loss that was caused by the hydroxyl group of APTES in the A-5 compound. A previous report showed that a compound filled with Closite 15A (Southern Clay) organoclay exhibited a fast vulcanization time because the large amount of ammonium salt in Closite 15A promoted the ring-opening rate of sulfur (S_8).[7]

The maximum torque values of the compounds increased in the order of A-2 < A-3 < A-1 < A-4 < A-5 < A-6. For the A-2 compound with pure Na^+-MMT, the dispersion of the clay within the rubber matrix was poor because of the hydrophilic properties of the clay. Accordingly, the accelerator could not participate in the crosslinking reaction and was adsorbed onto the layer-to-layer structure of clay, which decreased the degree of crosslinking in the SBR rubber. Therefore, the lowest value of the maximum torque was 1.76 N-m. The A-3 compound had a maximum torque value that was 0.23 N-m higher than the A-2 compound because the formation of covalent bonds between the hydroxyl group of Na^+-MMT and the ethoxy group of TESPT slightly improved the dispersion of the clay within the rubber matrix, and the degree of crosslinking increased as the tetrasulfide group of TESPT participated in the vulcanization process. The formation of agglomerates was reduced by the decreased polarity of the clay in the A-4 compound with APTES. Accordingly, as the amount of accelerator that cannot participate in the crosslink reaction decreased, the maximum torque value increased by 0.59 N-m over the A-2 compound. The maximum torque of the A-5 compound was 0.06 N-m higher than the A-4 compound. On the other hand, the A-6 compound was 0.55 N-m higher than the A-5 compound. Therefore,

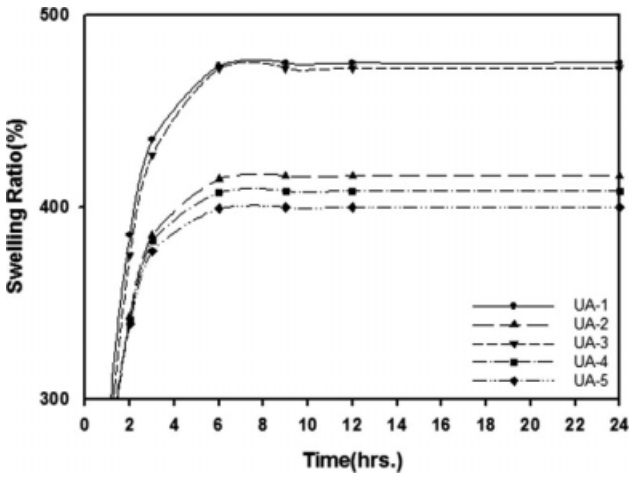

Figure 9 Swelling ratio of the various compounds for the unfilled system.

the A-6 compound exhibited better mechanical properties than the A-5 compound.

The delta torque values of the compounds increased in the order of A-2 < A-3 < A-4 < A-5 < A-1 < A-6. The delta torque value of the vulcanized rubber represented the degree of crosslinking that was caused by the chemical bonding between the molecules of the rubber and sulfur.[25] The degree of crosslinking was assumed to be the highest for the A-6 compound because it exhibited the largest difference in the delta torque value.

Swelling ratio of SBR and SBR/clay compounds

The degree of crosslinking was predicted from the swelling ratio measurements using toluene as a solvent in the Figures 9 and 10 and these values were compare to the values predicted from the delta torque data. The swelling ratio of all of the compounds leveled off after 9 h. After 24 h, the swelling ratios of the SBR compounds in the unfilled system decreased in the order of UA-1 (475%) > UA-3 (472%) > UA-2 (416%) > UA-4 (408%) > UA-5 (400%). This tendency was quite similar to the prediction data of the degree of crosslinking from the delta torque values of the cure characteristics data. The improvement in the degree of crosslinking was negligible for the UA-3 compound with APTES. However, the swelling ratio of the UA-4 compound with APTES and TESPT decreased by 8% compared to the UA-2 compound. Although the crosslink improvement effects of the chemical bonding between SBR and APTES were negligible when only APTES was added, the swelling ratio decreased because of the silanization between the ethoxy group of TESPT and the hydroxyl group of APTES when both APTES and TESPT were added. The crosslinking improved more for DDA than APTES because the UA-5 compound with DDA had the lowest swelling ratio.

The swelling ratio of the various compounds in the filled system decreased in the order of A-2 (521%) > A-1 (475%) > A-3 (424%) > A-4 (395%) > A-5 (366%) > A-6 (343%). For the A-2–A-6 compounds, the swelling ratio proportionally decreased as the delta torque value of the cure characteristics data increased. However, the unfilled A-1 compound did not follow this proportional correlation of the swelling ratio data. The dispersion of the silicates within the rubber matrix influenced the barrier properties of the filled compouns. The swelling ratio of the A-2 compound that was filled with unmodified MMT considerably increased by 13% compared to the A-1 compound because some of the accelerator was adsorbed onto the layer-to-layer of the clay and therefore, could not participate in the vulcanization, which reduced the degree of crosslinking. However, the swelling ratio of the A-3 compound with TESPT was lower than the A-1 and A-2 compounds because the tetrasulfide group of TESPT participated in the vulcanization reaction, increasing the degree of crosslinking. Additionally, the swelling ratio of the A-4 compound with APTES decreased by 32% compared to the A-2 compound because the accelerator loss was small for the clay agglomerates as the dispersion of the silicates improved through the formation of an intercalated structure of APTES in between the layers of the silicates. The swelling ratio of the A-5 compound decreased by 8% compared to the A-4 compound because the tetrasulfide group of TESPT and the reduction of the accelerator loss increased the degree of crosslinking. The swelling ratio of the A-6 compound considerably decreased by 38% and 7% respectively compared to the A-1 and A-5 compounds. From these results, the

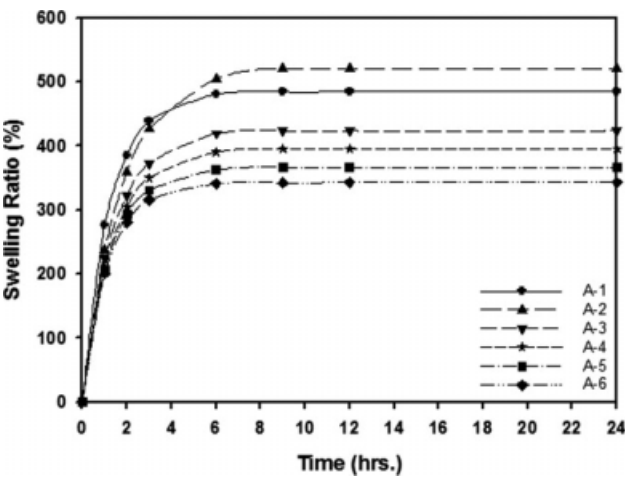

Figure 10 Swelling ratio of the various compounds for the filled system.

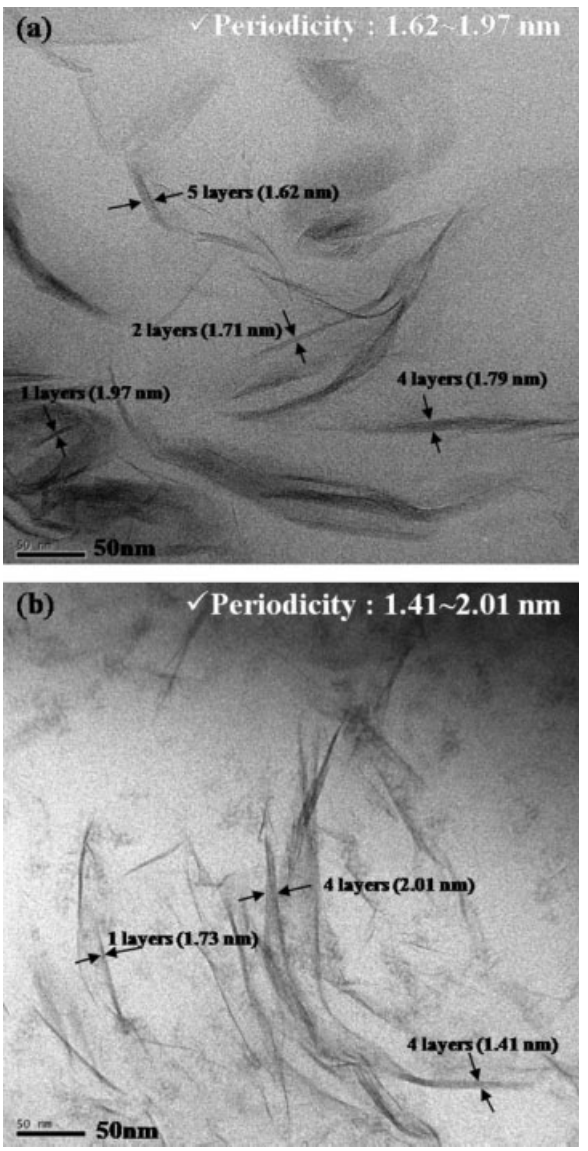

Figure 11 TEM images of the (a) SBR/APTES-MMT and (b) SBR/DDA-MMT nanocomposites after coagulation (dry sample).

ammonium ions of DDA improved the crosslinking more than APTES.

TEM morphology

Figure 11 shows the TEM images of SBR/APTES-MMT and SBR/DDA-MMT after coagulation (dry sample). The aggregate state of the silicates and the layer-to-layer distance were determined from these images. Between 2 and 8 silicate layers were aggregated for SBR/APTES-MMT, and the aggregates were quite well dispersed in the SBR matrix. The layer-to-layer distance was 1.62–1.97 nm, corresponding to 2θ values of 5.45–4.48°, which were consistent with the XRD pattern in Figure 5(a). Between 2 and 4 silicate layers were aggregated for SBR/DDA-MMT, and the aggregates were well dispersed. The layer-to-layer distance was 1.41 nm (6.27°)–2.01 nm (4.30°) which corresponded well to the XRD pattern in Figure 5(b). Figure 12 shows the TEM images of the SBR/clay nanocomposites that were made using Na-MMT, APTES-MMT, and DDA-MMT. In Figure 12(a), the silicates of the SBR/Na-MMT was not well dispersed because 15–16 layers of the silicates were reaggregated because a strong reaggregation effect was caused by the polarity of the silicates during the coagulation process even though the clay was exfoliated in the swelling process.[17] In contrast, the dispersion of the silicates improved within the rubber matrix for the SBR/organoclay nanocomposites that were made using APTES and DDA. Between 2 and 8 silicate layers of silicates were aggregated in the SBR/APTES-MMT nanocomposites because the silicate surface became less polar either through the cation exchange reaction between the Na^+ ions between the silicate layers and the ammonium ions of APTES or the ion-polar interaction between the Na^+ ions or the oxygen atoms of the silicates and the hydroxyl group of APTES. Accordingly, the dispersion of the silicates within the rubber matrix improved as the reaggregation of the silicates weakened through the coagulation process because of the decreased polar–polar interaction between the layers of the silicate. Additionally the dispersion of the silicates within the rubber matrix further improved for the SBR/DDA-MMT nanocomposites through formation of 2–4 silicate layers of aggregates. The silicate surfaces of APTES-MMT exhibited some polarity because of the hydroxyl group created by APTES. On the other hand, the reaggregation effect was more weakened as polarity of the silicate surface decreased through the introduction of hydrophobic DDA in DDA-MMT. Accordingly, the exfoliated structure was not observed in the XRD data for DDA-MMT because the dispersion of the silicates was very good within the rubber matrix. The dispersed silicates in Figure 12(c) were darker than Figure 12(b). Therefore, the layer-to-layer distance of DDA-MMT was shorter than APTES-MMT because the silicates were aggregated through the cation exchange reaction between the H^+ ions and the Na^+ ions in the silicates. The dispersion of the silicates within the rubber matrix improved for both the SBR/organoclay nanocomposites that were modified with APTES and DDA. However, the dispersion of silicates was further improved when DDA was used as the modifier.

Mechanical properties

The 100 and 300% modulus (M_{100} and M_{300}), the tensile strength, and the elongation at failure were measured to determine the effects of APTES, DDA

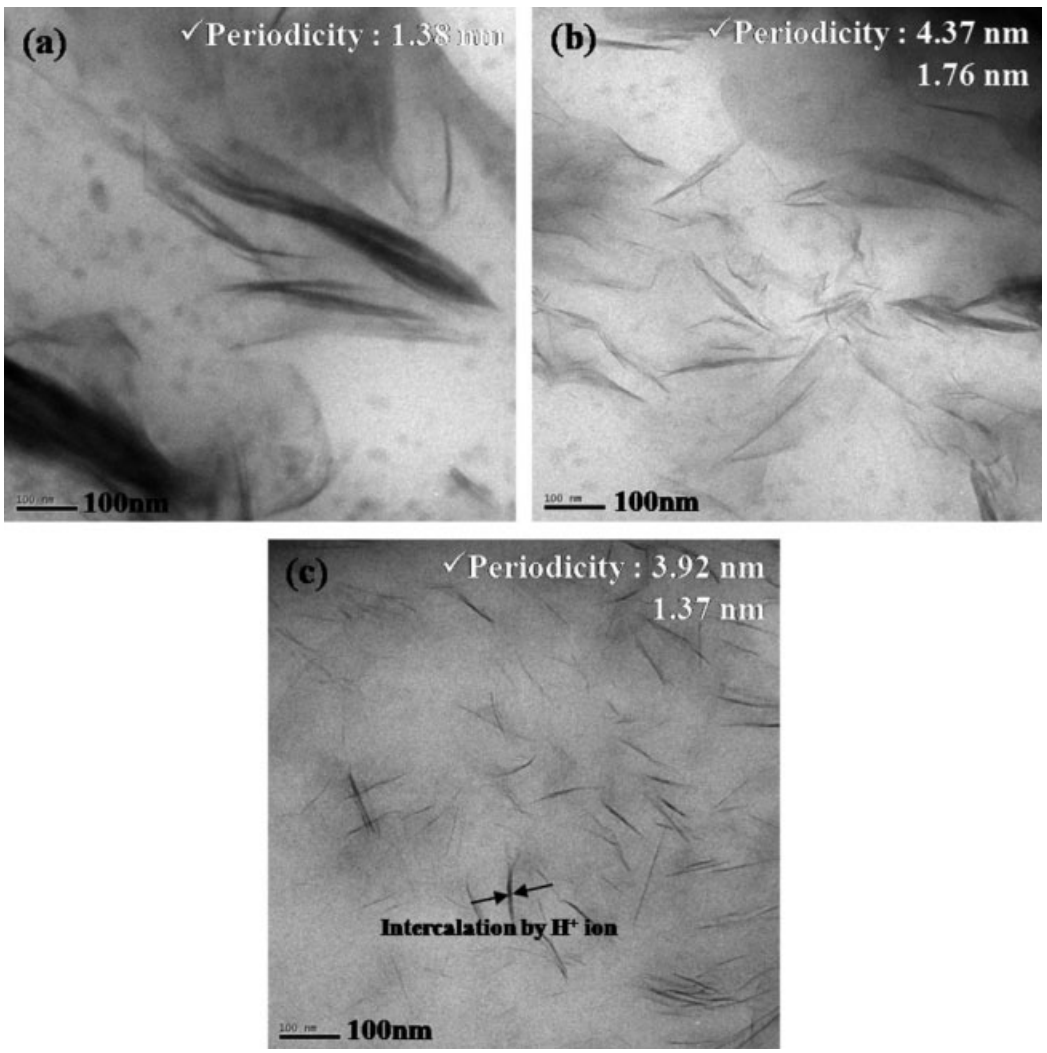

Figure 12 TEM images of the (a) SBR/Na-MMT, (b) SBR/APTES-MMT and (c) SBR/DDA-MMT nanocomposites after vulcanization.

and TESPT on the mechanical properties of the SBR compound in the unfilled system, and the results are shown in Table III. The 100 and 300% modulus increased in the order of UA-1 < UA-3 < UA-2 < UA-4 < UA-5, showing a proportional correlation with the swelling ratio. The modulus improved as the degree of crosslinking increased. The 100 and 300% modulus values of the UA-3 compound increased slightly in comparison to the pure SBR compound. Therefore, the improvement in the mechanical properties that was caused by the chemical bonding of APTES was negligible. The mechanical properties of the UA-2 compound were higher than the pure SBR compound because of the degree of crosslinking that was caused by the tetrasulfide group of TESPT. The 300% modulus values of the UA-4 and UA-5 compounds increased by 4.5 and 9.5%, respectively, compared to the UA-2 compound and the elongation decreased by 1.1 and 8.0%, respectively. The tensile strengths of these compounds were similar. Accordingly, for the UA-4 compound with both APTES and TESPT, the

TABLE III
Tensile Properties of the SBR Compounds for the Unfilled System

No.	Items	UA-1	UA-2	UA-3	UA-4	UA-5
1	M_{100} (MPa)	1.06	1.15	1.08	1.26	1.30
2	M_{300} (MPa)	1.62	2.01	1.67	2.10	2.20
3	Tensile strength (MPa)	1.87	2.37	1.95	2.42	2.41
4	Elongation (%)	379	361	378	357	332

TABLE IV
Tensile Properties of the SBR and SBR/Clay Compounds for the Filled System

No.	Items	A-1	A-2	A-3	A-4	A-5	A-6
1	M_{100} (MPa)	1.09	1.42	1.48	1.59	1.85	2.07
2	M_{300} (MPa)	1.76	3.03	3.71	4.26	5.09	5.67
3	Tensile strength (MPa)	2.01	3.73	4.73	6.08	6.79	6.78
4	Elongation (%)	368	458	424	458	418	373

elongation decreased as the modulus increased. However, this elongation change was smaller than the case of UA-5 compound, which contained both DDA and TESPT. The UA-5 compound exhibited the highest 100 and 300% modulus values.

The mechanical properties of the SBR/organoclay compounds are provided in Table IV. The 100 and 300% modulus increased in the order of A-1 < A-2 < A-3 < A-4 < A-5 < A-6. Reduced mechanical properties were anticipated for the A-2 compound because the swelling ratio was 6.9% higher than the A-1 compound, but the results were not consistent with this theory because the unique plate-like structure of Na^+-MMT distributed within the rubber matrix using the latex method caused hydrodynamic reinforcing effects. When TESPT was added to the A-2 compound to form the A-3 compound, the dispersion of the clay improved because of the chemical bonding between the hydroxyl group on the side surface of the clay and the ethoxy group of TESPT. Additionally, the A-3 compound exhibited better mechanical properties than the A-2 compound because its crosslink was improved by the tetrasulfide group of TESPT. The 100 and 300% modulus and the tensile strength of the A-4 compound with APTES were better than the A-3 compound with TESPT the silicate dispersion effects of APTES were more significant than the higher degree of crosslinking caused by TESPT. The 300% modulus and tensile strength of the A-5 compound increased by 20 and 12%, respectively, compared to the A-4 compound, whereas the elongation decreased by 9% because the tetrasulfide group of TESPT increased the crosslinking in the SBR/APTES-MMT nanocomposites. the 300% modulus of the A-6 compound increased by 11% compared to the A-5 compound, whereas the tensile strengths were similar. Additionally, the elongation decreased by 11%. Thus, the degree of crosslinking in the A-6 compound was higher than the A-5 compound. Therefore, the SBR/organoclay compound made using DDA exhibited better mechanical properties the SBR/organoclay compound made using APTES.

Dynamic viscoelastic behavior

Figure 13 shows the dynamic viscoelastic behavior of the uncured SBR/organoclay compound with respect to the strain sweep. The Payne effect was the change in the storage modulus (E') behavior the dynamic strain was repeatedly applied and was caused by the changes in filler–filler network or reaggregation.[26-28] In Figure 13, the typical nonlinear behavior of the Payne effect was observed as the storage modulus decreased with increasing strain amplitude. For the A-1 compound of the unfilled rubber, the storage modulus exhibited almost no change as the strain amplitude increased. In contrast, the A-2 compound filled with clay had a high storage modulus at small strains, but the storage modulus rapidly decreased along as the strain amplitude increased because the filler-rubber interaction was weak, and the filler–filler interaction was very strong. According to the Payne effect, the filler network increases as the aggregates transform into agglomerates, and generally, the dynamic strain breaks the network between these agglomerates.[26,27]

However, for the A-3 compound with TESPT added to the SBR/clay compound, the storage modulus was relatively low at small strains compared to the A-2 compound. The miscibility with the SBR rubber improved as the polarity of the silicates decreased because of the chemical bonding between the hydroxyl group on the surface of the silicates and the ethoxy group of TESPT. As a result, the filler–filler interaction reduced more than the A-2 compound. A previous report showed that the storage modulus of the SBR/silica compound with TESPT

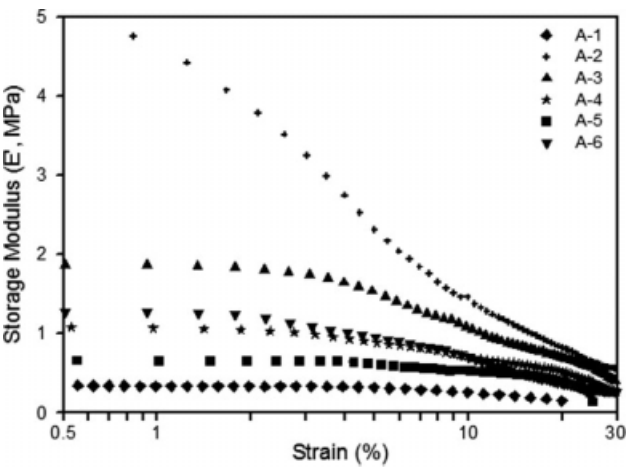

Figure 13 Strain dependence of the storage modulus for the uncured SBR/organoclay nanocomposites.

was lower the same compound without TESPT at small strains because of the chemical bonding between the hydroxyl group on the surface of silica and the ethoxy group of TESPT.[29] The A-6 compound had a higher storage modulus than the A-4 compound because APTES was well adsorbed onto the surface of the silicate through polar interactions. Therefore, the decrease in the filler–filler interaction was more significant for APTES than DDA.

The A-5 compound with TESPT added to the SBR/APTES-MMT compound had the second lowest storage modulus, which was almost constant as a function of the strain. Additionally, the storage modulus value of the A-5 compound was smaller than the A-4 compound without TESPT. Therefore, chemical bonds formed between the hydroxyl group from APTES on the silicate surface APTES and the ethoxy group of TESPT, which decreased the filler–filler interaction.

Figure 14 shows the dynamic viscoelastic properties with respect to changes in the temperature of the vulcanized SBR/organoclay nanocomposites. In the temperature range of −60 to 80°C, in Figure 14(a), the storage modulus curves of the A-2, A-5, and A-6 compounds shifted to the right more than the unfilled SBR compounds, showing an increase in the storage modulus with respect to the strain amplification of the rubber molecules attached to the filler surface. For the polymers that were filled with carbon black or organic pigments, the whole modulus curve shifted to the right with increasing temperature at a fixed frequency.[30]

For the unfilled compounds in the glass transition region, the storage modulus began to decrease at slightly higher temperatures for the UA-4 and UA-5 compounds compared to the A-1 compound. Similar to the swelling ratio results, the movement of the SBR molecule chain was restricted for the UA-4 and UA-5 compounds because their degrees of crosslinking were higher than the pure SBR compound. Additionally, for the A-2 compound that was not organically treated, the storage modulus started to decrease at a lower temperature than the A-5 and A-6 compounds because of the lowering degree of crosslinking and the weakened interaction between the rubber molecule chain and the clay.

In Figure 14(b), a loss factor (tan δ) was measured the temperature changed from the glass transition region to the rubbery region. The T_g was determined from the tan δ peak and increased in the order of A-1 (−37.4°C) < UA-4 (−36.4°C) < A-2 (−35.3°C) ≈ UA-5 (−35.3°C) < A-6 (−31.8°C) < A-5 (−30.8°C). For the unfilled SBR compounds, the T_g value of the UA-4 compound was 0.9°C higher than the UA-4 compound. Therefore, the movement of the SBR molecule chain was restricted by the increased degree of crosslinking, which was identical to the

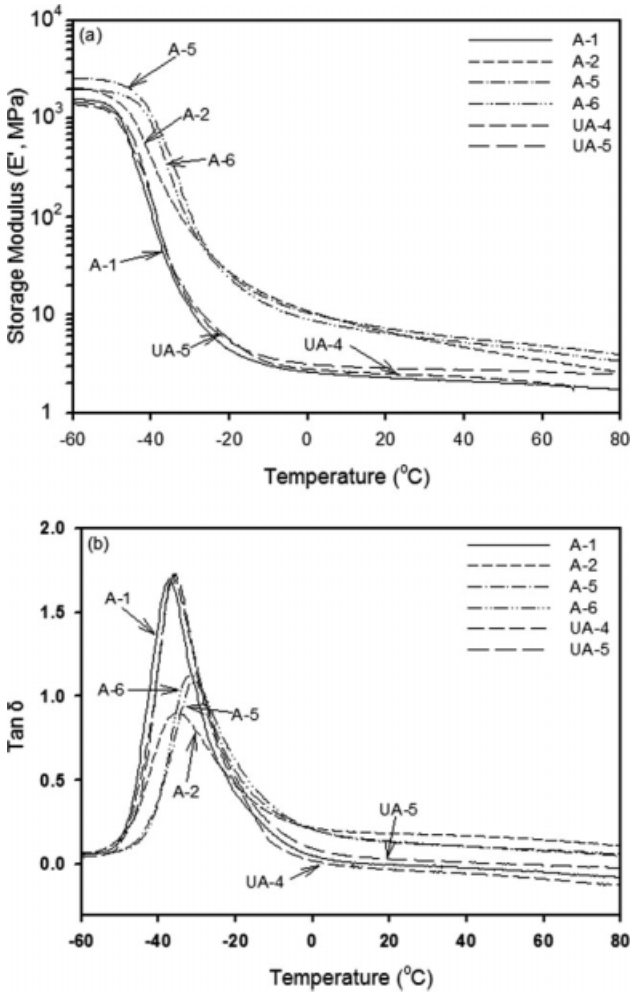

Figure 14 Temperature dependence of (a) the storage modulus (E') and (b) the loss tangent for the unfilled SBR compounds and the SBR/organoclay nanocomposites after vulcanization.

the degrees of crosslinking that were predicted by the swelling ratio results. However, the A-5 and A-6 compounds that were filled with organoclay, exhibited opposite tendencies from the swelling ratio results. The T_g value of the A-5 compound was 1°C higher than the A-6 compound because the viscous properties of the A-6 compound were higher than the A-5 compound causing a slight increase of the tan δ value in the glass transition region.

In the glass transition zone of the polymer at low temperatures (−60 to −20°C), the main portion of the composite was the polymer matrix for the energy dissipation because the filler network was not easily broken down.[26,27,31,32] Additionally, in the rubbery region of the polymer at high temperatures (higher than 20°C), the main portion of the composite was the filler–filler interaction for the energy dissipation.[26,27,31,32] For the SBR compound filled with carbon black loaded from 0 to 70 phr, the intensity of tan δ peak decreased by as the concentration in

rubber matrix increased in the glass transition region of the polymer possibly because of the decrease in the effective volume of polymer as the amounts of filler in SBR compound increased.[26,27] Additionally, the tan δ peak intensity of the SBR/clay compound decreased as the effective volume of polymer decreased in the glass transition region because as the amount of trapped rubber increased.[31,32] The hydrophilic clay within the rubber matrix formed aggregates or agglomerates.[31,32]

The tan δ value was defined in terms of the viscous component divided by the elastic component. The A-5 and A-6 compounds, with a modifier and TESPT, exhibited relatively higher tan δ values than the A-2 compound in the glass transition region. Therefore, viscosity of the rubber matrix increased through the addition of a modifier and TESPT. The SBR compounds with TESPT had higher tan δ values than the compounds without TESPT in the glass transition region of the polymer because TESPT increased the viscous properties of the rubber matrix.[4] However the A-2 compound had the highest tan δ value in the rubbery region. The tan δ values of SBR/clay compound was higher than the SBR/organoclay compounds at temperatures over 20°C.[31] Therefore, the energy loss of the strong filler–filler network at small strains was relatively higher than the A-5 and A-6 compounds.

CONCLUSIONS

For the manufacture process of SBR/organoclay nanocomposites using the latex method, the XRD results showed that Na^+-MMT was exfoliated in a water suspension, and the layer-to-layer distance increased up to 1.81 nm after coagulation. SBR particles were not present in between the silicates because the particle size distribution was between 20 and 162 nm. The cake on the filter paper was evaluated, and the APTES molecules were adsorbed onto the silicate surface through the ion-polar interaction between the hydroxyl group of APTES and the silicates, when APTES and the MMT suspension were mixed. On the other hand, an ion-polar interaction did not existed between the silicate and DDA. After coagulation, a peak appeared at 6.2° for the DDA modifier because of the cation exchange reaction between the H^+ ionsand the Na^+ ions in the silicates. The XRD peaks and TEM images showed that the dispersion of the silicates improved for both APTES-MMT and DDA-MMT. In the manufacturing process of the SBR/organoclay nanocomposites using the latex method, the number of aggregated silicate layers was influenced by the degree of polarity for the silicates, and the polarity was altered by the modifier. In this experiment, the nanocomposites had 2–8 layers when APTES was used and 2–4 layers when DDA was used. The dispersion within the rubber matrix was better for hydrophobic DDA compared to APTES-MMT. The SBR/organoclay compounds exhibited fast cure rates than the SBR/clay compounds because well dispersed silicates reduced the amount of accelerator that was adsorbed. In the filled system, the scorch time of the SBR/APTES-MMT compound was delayed because of the influence of the hydroxyl group on the silicate surface that was generated by APTES. The SBR/DDA-MMT compound had the fastest scorch time, optimal vulcanization time and cure rate. Additionally, the SBR/DDA-MMT compound exhibited less accelerator loss compared to APTES and promoted crosslinking because of the presence of the amine. The SBR/DDA-MMT compound had the lowest swelling ratio, and its degree of crosslinking was the highest. When considering A-3 and A-4 compound, the effect of the dispersion of the silicates in the rubber matrix caused by the modifiers was more significant to the tensile properties of the SBR/organoclay nanocomposites than the increase in the degree of crosslinking caused by TESPT. The storage modulus values of the uncured compounds reduced than when TESPT was added to the SBR/APTES-MMT compound. This means that a covalent bond formed between the hydroxyl group of APTES and the ethoxy group of TESPT. From the behavior of the tan δ of the cured compounds with respect to temperature changes, the SBR/organoclay nanocomposites exhibited decreased filler–filler interactions in the rubbery region.

Consequently, the mechanical properties of the SBR/organoclay nanocomposites improved more with the DDA modifier than with APTES modifier because the degree of crosslinking and the dispersion of the silicates within the rubber matrix were relatively higher for DDA even though the APTES modifier formed a covalent bond with TESPT.

References

1. Findik, F.; Yilmaz, R.; Köksal, T. Mater Des 2004, 25, 269.
2. Fröhlich, J.; Niedermeier, W.; Luginsland, H.-D. Compos A 2005, 36, 449.
3. Hui, R.; Yixin, Q.; Suhe, Z. Chin J Chem Eng 2006, 14, 93.
4. Valentin, J. L.; Mora-Barrantes, I.; Rodriguez, A.; Ibarra, L.; Gonzalez, L. J Appl Polym Sci 2007, 103, 1806.
5. Son, M. J.; Kim, W. Elastomer 2006, 41, 260.
6. Kim, W.; Kim, S. K.; Kang, J. H.; Choe, Y. Macromol Res 2006, 14, 187.
7. Kim, W.; Kang, B. S.; Cho, S. G.; Ha, C.; Bae, J. W. Compos Interface 2007, 14, 409.
8. Jia, Q.; Wu, Y.; Wang, Y.; Lu, M.; Zhang, L. Compos Sci Technol 2008, 68, 1050.
9. Brigatti, M. F.; Galan, E.; Theng, B. K. G. Handbook of Clay Science; Bergaya, F.; Theng, B. K. G.; Lagaly, G., Eds.; Elsevier: Netherlands, 2006; Chapter 2, pp 19–44.
10. Wang, Y.; Zhang, L.; Tang, C.; Yu, D. J Appl Polym Sci 2000, 78, 1879.

11. Lebaron, P. C.; Wang, Z.; Pinnavaia, T. J. Appl Clay Sci 1999, 15, 11.
12. Ma, J.; Xiang, P.; Mai, Y. W.; Zhang, L. Q. Macromol Rapid Commun 2004, 25, 1692.
13. Wang, Y. Q.; Zhang, H. F.; Wu, Y. P.; Wang, J.; Zhang, L. Q. Presented at the Symposium of International Rubber Conference; Rubber Institute, Chemical Industry and Engineering Society of China: Beijing, China, Sept. 21–25, 2004, Vol B, p 420.
14. Zhang, H. F.; Wang, Y. Q.; Wu, Y. P.; Zhang, L. Q.; Yang, J.; Wang, X. F. Presented at the Symposium of International Rubber Conference; Rubber Institute, Chemical Industry and Engineering Society of China: Beijing, China, Sept. 21-25, 2004, Vol B, p 240.
15. Wu, Y.; Jia, Q.; Yu, D.; Zhang, L. J Appl Polym Sci 2003, 89, 3855.
16. Zhang, L. Q.; Wang, Y. Z.; Wang, Y. Q.; Sui, Y. A.; Yu, D. S. J Appl Polym Sci 2000, 78, 1873.
17. Wu, Y.; Wang, Y.; Zhang, H.; Wang, Y.; Yu, D.; Zhang, L.; Yang, J. Compos Sci Technol 2005, 65, 1195.
18. Wang, Y.; Zhang, H.; Wu, Y.; Yang, J.; Zhang, L. Eur Polym J 2005, 41, 2776.
19. Kim, W. S.; Lee, D. H.; Kim, I. J.; Son, M. J.; Cho, S. G.; Kim, W. Macromol Res 2009, 17, 776.
20. Galimberti, M.; Senatore, S.; Conzatti, L.; Costa, G.; Giuliano, G.; Guerra, G. Polym Adv Technol 2009, 20, 135.
21. Ciullo, P. A.; Hewitt, N. The Rubber Formulary; Noyes Publications: New York, 2003; pp 28–32.
22. Lan, T.; Kaviratna, P. D.; Pinnavaia, T. J. Chem Mater 1994, 6, 573.
23. Mark, J. E.; Erman, B.; Eirch, F. R., Eds. Science and Technology of Rubber, Academic Press: New York, 1978; p 291
24. Mousa, A.; Karger-Kocsis, J. Macromol Mater Eng 2001, 286, 260.
25. Mandal, S. K.; Basu, D. K. Rubber Chem Technol 1994, 67, 672.
26. Wang, M. J. Rubber Chem Technol 1998, 71, 520.
27. Wang, M. J. Rubber Chem Technol 1999, 72, 430.
28. Payne, A. R.; Whittaker, R. E. Rubber Chem Technol 1971, 44, 440.
29. Wu, Y.; Zhao, Q.; Zhao, S.; Zhang, L. J Appl Polym Sci 2008, 108, 112.
30. Kraus, G.; Rollmann, K. W.; Gruver, J. T. Rubber Chem Technol 1971, 44, 598.
31. Meneghetti, P.; Shaikh, S.; Qutubuddin, S.; Nazarenko, S. Rubber Chem Technol 2008, 81, 821.
32. Schön, F.; Thomann, R.; Gronski, W. Macromol Symp 2002, 189, 105.